Chapter 9

Properties of LCS

The preceding chapters have illustrated the effectiveness of using the FTLE-LCS method for revealing transport mechanisms in geophysical flows, and in flows defined by a dynamical system. In other fields, researchers are harnessing the utility of the method for revealing coherent structures in a wide array of aperiodic flows. However, the number of papers dealing with the theoretical underpinnings of FTLE and LCS has not grown proportionately. Since Haller's original inception of the idea [Haller 2000, Haller 2001], excellent contributions to the theory of LCS have been provided by [Shadden 2005] and [Lekien 2007], which provide rigorous definitions for LCS that had not previously been codified, as well as a bound for the amount of flux that crosses the LCS. Haller has also explored the robustness of LCS to noise in the velocity field [Haller 2002], and used the premise of LCS to analyze criteria for separation in unsteady flows in [Surana 2008, Weldon 2008]. Motivated by applications, several groups have also provided an equivalent LCS theory for inertial particles in a flow [Sapsis 2009, Tallapragada 2008, Peng 2009]. This being said, the literature contains very little analysis on the fundamental *properties* of LCS – that is, given a rigorous definition of the LCS, what properties follow from this definition?

In tandem with this want of rigorous theoretical results, there have been, in the LCS literature over the last decade, tacit assertions made regarding the properties of LCS. In many cases, these assertions have been made as a pedagogical tool to illustrate an idea by analogy; however, many end users of the theory have consequently attributed these properties as statements of fact. To be sure, the proponents of LCS

theory have not made errors in their analysis. However, in the presentation of ideas, these assertions have often been propagated. Indeed, there is hardly a published paper utilizing the LCS method that does not make these assertions to some degree.

Most commonly, the assertions to which we are referring are the following:

A1. The repelling/attracting LCS generalize stable/unstable manifold theory from autonomous flows to aperiodic flows.

A2. LCS are invariant, or stated differently, the LCS are material surfaces.

In this chapter, we will investigate the LCS in relation to these two properties. The approach will use both analysis and examples to illustrate the ideas, and to provide direct counterexamples.

One reason for the slow development of a theory surrounding LCS beyond the applications is the lack of readily available approaches for analysis. As we have seen, the LCS is defined in terms of the derivatives of the flow map, whereas, for the analysis we would like to determine properties of the LCS in terms of the underlying velocity field. For the aperiodic flows we are considering, the flow map can only be determined by numerical integration. Moreover, the LCS is defined in terms of a derivative condition on the flow map, and verification of the properties of the LCS requires access to the derivatives of this condition.[1] With this in mind, this thesis does not claim to provide the needed breakthrough in the analysis. It is hoped, however, that an informed discussion of these issues will help to provide a more rigorous framework in which to continue development of FTLE-LCS theory.

We proceed by addressing each of the previously stated assertions in turn. The final section of this chapter will then investigate the possibility of an evolution equation for the LCS in terms of the underlying velocity field.

[1]The difficulty of the situation can be appreciated anecdotally by referring to a conversation of the author with Dr. Peter Constantin, of the University of Chicago, who, after hearing of the attempt to provide further analysis for LCS, and realizing the need to come to terms with the flow map with arbitrary time dependence, exasperatedly exclaimed: “Heaven help you!”.

9.1 LCS and stable and unstable manifolds

Recall that, given a hyperbolic fixed point, p, in an autonomous velocity field, the stable and unstable manifolds of p are defined as the union of points whose trajectories asymptote toward p as $t \to \infty$ and $t \to -\infty$, respectively. Even in this thesis, we have seen applications in which the correspondence between LCS and stable/unstable manifolds appears very convincing. In our very first example (the simple pendulum of Chapter 3), the LCS appears to coincide precisely with the well-known stable and unstable manifolds for pendulum flow. Even the fact that the LCS "grow" away from the fixed point as the integration time, T, is increased, is suggestive of the definition of stable and unstable manifolds. Further examples in this thesis have used the LCS method to reveal homoclinic tangle structures in a variety of aperiodic flows that unmistakably resemble the stable and unstable manifolds of Poincaré maps associated with periodically forced flows. Further evidence for the link between LCS and manifolds is the observation that stable and unstable manifolds traditionally define *separatrices* in a time-independent flow, just as has been shown for LCS which, *by definition*, are surfaces of greatest separation. In addition, the property that stable and unstable manifolds are invariant manifolds seems to be true for LCS computed numerically in physical flows (although this property will be examined more closely in the next section.)

Given the aforementioned observations, it is understandable that analogies have been made between LCS and stable/unstable manifolds, leading prematurely to the conclusion that LCS represent the generalizations of these manifolds from autonomous flows to aperiodic flows. For this claim to be true, there needs to be a mathematical link between asymptotic trajectories (in the definition of manifolds) and separation (in the definition of LCS). We shall now see through example that this link does not hold necessarily, and that an important criterium to monitor in this regard is the rate of separation along the unstable manifold.

Before proceeding, we introduce the following definitions that will be useful when discussing the examples:

Definition: Let $\mathbf{u}(\mathbf{x})$ be an autonomous velocity field defined on $\mathbb{R}^2$ that has a hyperbolic fixed point, $\mathbf{p} \in \mathbb{R}^2$. Denote the one-dimensional invariant unstable manifold of $\mathbf{p}$ as $W^u(\mathbf{p})$. For a point $\mathbf{x}_0^u \in W^u(\mathbf{p})$, let $\mathbf{x}^u(t, \mathbf{x}_0^u)$ denote the solution trajectory parameterized by time for which $\mathbf{x}^u(0, \mathbf{x}_0^u) = \mathbf{x}_0^u$. Let $s(t; \mathbf{x}_0^u)$ be the arclength along the trajectory $\mathbf{x}^u(t; x_0)$ also parameterized by time, so that $s(0; \mathbf{x}_0^u) = 0$, and $s(t; \mathbf{x}_0^u)$ is a strictly increasing function in t. Then, for $T > 0$, the unstable manifold $W^u(\mathbf{p})$ is said to be

- *sublinear* up to time T if

$$\frac{d^2}{dt^2} \ln s(t, \mathbf{x}_0^u) < 0 \tag{9.1}$$

- *superlinear* up to time T if

$$\frac{d^2}{dt^2} \ln s(t, \mathbf{x}_0^u) > 0 \tag{9.2}$$

- *linear* up to time T if

$$\frac{d^2}{dt^2} \ln s(t, \mathbf{x}_0^u) = 0 \tag{9.3}$$

for all $t \in [0, T]$, and for all $\mathbf{x}_0^u$ in some neighborhood of p.

By choosing T small enough, every unstable manifold can be assigned one of these definitions.

Example 1. Flow near a linear saddle: The quintessential flow that exhibits stable and unstable manifolds in an autonomous flow is the linear saddle. Consider the linear flow in the coordinates $\mathbf{x} = (x, y)$ prescribed by

$$\dot{\mathbf{x}} = A\mathbf{x}\,, \qquad\qquad A := \begin{bmatrix} 1 & 0 \\ 0 & -1 \end{bmatrix}. \tag{9.4}$$

The streamlines for this flow are plotted in Figure 9.1. In this case, we can solve for

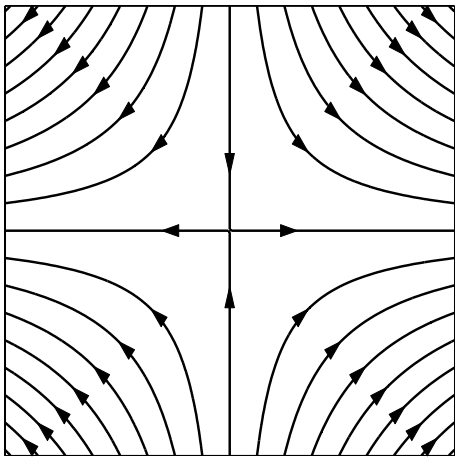

Figure 9.1: Streamlines in the flow of a linear saddle.

the flow map, and the FTLE analytically. An initial condition, $\mathbf{x}_0 = (x_0, y_0)$, mapped forward in the flow becomes

$$\mathbf{x}(t_0 + T) = \begin{bmatrix} x_0 e^T \\ y_0 e^{-T} \end{bmatrix} . \tag{9.5}$$

The linearization of the flow map is

$$\left. \frac{d\phi_{t_0}^{t_0+T}}{d\mathbf{x}} \right|_{\mathbf{x}=\mathbf{x_0}} = \begin{bmatrix} e^T & 0 \\ 0 & e^{-T} \end{bmatrix} , \tag{9.6}$$

and the deformation tensor is

$$\Delta = \begin{bmatrix} e^{2T} & 0 \\ 0 & e^{-2T} \end{bmatrix} . \tag{9.7}$$

Finally, following the definition in (3.3), the FTLE is

$$\sigma(\mathbf{x}, t) = 1 . \tag{9.8}$$

The FTLE is constant in both space and time, and hence admits neither ridges nor LCS. This result is, of course, not surprising since the flow map itself is independent of

both space and time. We conclude that all points in the flow separate at an equal rate, regardless of their initial location with respect to the stable and unstable manifolds; in particular, initial conditions straddling the stable manifold separate at the same rate as all other trajectories in the flow. In effect, all particles are slaved to the unstable manifold and separation of particles along the unstable manifold is uniform. This trivial example indicates that *LCS computed using FTLE cannot generalize stable and unstable manifolds to aperiodic systems since we have an example in which LCS do not reduce to the stable and unstable manifolds in the autonomous case.*

In terms of the definitions provided above, the unstable manifold in this example is *linear* and represents a critical case. Insight is gained by examining two further examples that represent *sublinear* and *superlinear* cases.

Example 2. Flow due to two point vortices: Consider the potential flow generated by two point vortices with equal and opposite vorticity located at $(-a, 0)$ and $(a, 0)$ in the plane with constant $a > 0$. The stream function describing the flow in a reference frame translating with the vortices is

$$\psi(x, y) = \frac{1}{2\pi}\left[\frac{x}{2a} + \ln\left(\frac{r_2}{r_1}\right)\right], \tag{9.9}$$

where r_1 and r_2 are the distances from the point (x, y) to the first and second vortices, respectively. The stream function for this autonomous flow is shown in Figure 9.2(a), and the velocity field generated by this stream function is

$$\begin{aligned}\dot{x} &= \frac{1}{2\pi}\left(\frac{y}{r_2^2} - \frac{y}{r_1^2}\right)\\ \dot{y} &= \frac{1}{2\pi}\left(\frac{x+a}{r_1^2} - \frac{x-a}{r_2^2} - \frac{1}{2a}\right).\end{aligned}$$

The flow exhibits two hyperbolic fixed points along the y-axis, and the stable and unstable manifolds associated with these fixed points are well-defined. The heteroclinic manifolds joining the fixed points are separatrices that delineate the region of fluid that translates with the vortex, while fluid outside the heteroclinc connection

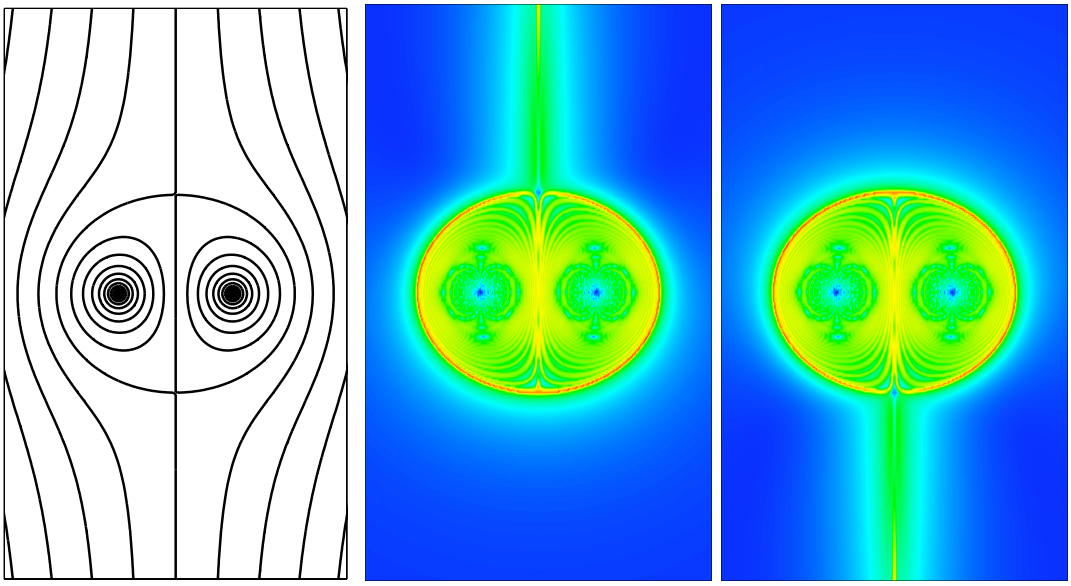

(a) Streamlines. Bulk flow is from top to bottom.

(b) Repelling FTLE.

(c) Attracting FTLE.

Figure 9.2: LCS in the flow of the double point vortex flow. The repelling and attracting LCS coincide with the stable/unstable manifolds.

appears to move downward and out of the field of view.

The corresponding FTLE fields for this flow computed numerically are shown in 9.2(b) and 9.2(c). The bulk flow outside the vortex is a largely uniform flow in which there is no separation and the deformation tensor is zero. Hence, the largest separation occurs between the flow inside the vortex and the bulk flow, and consequently the LCS does indeed agree with the stable and unstable manifolds. For this example, the stable and unstable manifolds coincide with the LCS, and is a case in which the velocity field along the unstable manifold is *sublinear*.

Example 3. Flow in Hill's vortex: In an 1884 monograph (see reference at [Hill 1894]), Hill considered a three-dimensional flow with an axis of symmetry. Taking the z-axis as the axis of symmetry, and using cylindrical coordinates (r, θ, z), he showed that level surfaces defined by

$$r^2\left(r^2 + z^2 - 1\right) = \text{constant} \tag{9.10}$$

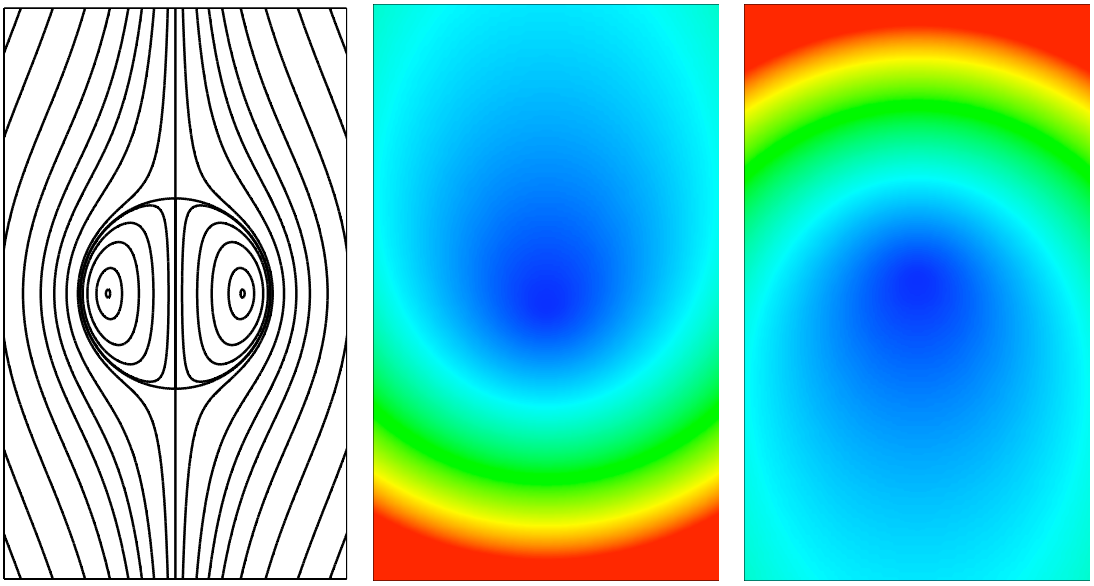

(a) Streamlines. Bulk flow is from top to bottom.

(b) Repelling FTLE.

(c) Attracting FTLE.

Figure 9.3: LCS in the flow of Hill's spherical vortex. The FTLE fields admit neither ridges nor LCS.

are invariant surfaces under the axisymmetric flow defined by[2]

$$\dot{r} = 2rz \tag{9.15}$$

$$\dot{\theta} = 0 \tag{9.16}$$

$$\dot{z} = -2(2r^2 - 1) - 2z^2 \,. \tag{9.17}$$

Figure 9.1 shows the streamlines (invariant surfaces) on a planar section of the flow through the axis of symmetry. The streamline patterns are very similar to those

[2]Hill's result was actually more general than this. He showed that the level surfaces of

$$r^2 \left(\frac{r^2}{a^2} + \frac{(z-Z)^2}{c^2} - 1 \right) = \text{constant} \tag{9.11}$$

are invariant under the flow

$$\dot{r} = 2\frac{k}{c^2} r(z - Z) \tag{9.12}$$

$$\dot{\theta} = 0 \tag{9.13}$$

$$\dot{z} = -2\frac{k}{a^2}(2r^2 - a^2) - 2\frac{k}{c^2}(z - Z)^2 \tag{9.14}$$

for arbitrary constants a, c, and k, and any function of time Z.

for the previous flow arising from two point vortices – the geometric structure of the stable and unstable manifolds are identical. However, the important difference is that the bulk flow *accelerates superlinearly* as it travels in the direction of the negative z-axis, and the z-coordinate of the flow becomes infinite in finite time – the culprit being the $-z^2$ term in the z-component of the velocity.

Although the structure of the stable and unstable manifolds of the Hill vortex flow and the point vortex flow are identical, the FTLE fields are very different. The FTLE fields for the Hill vortex are shown in Figure 9.3. The FTLE has a smooth gradient that does not admit ridges – *there are no LCS in this flow.* Particles initially located further down the negative z-axis experience larger separation in a fixed amount of time. Hence, separation in the flow is not at all related to the location of stable and unstable manifolds. Separation along the unstable manifold in this example is *superlinear.*

Reviewing the results in these three examples, we can conclude that flows must be sublinear for the repelling LCS to correspond with the stable manifold, and likewise the attracting LCS with the unstable manifold. Otherwise, the faster than exponential rate of stretching ensures that the greatest rate of separation will not occur at the stable manifold.

We can attribute the fact that excellent agreement of the LCS with stable and unstable manifolds has been routinely found in physical flows (such as oceans, atmospheres, laboratory flows, etc.) to the observation that flows in these applications are physical and characteristically sublinear; the rate of separation along unstable manifolds does not grow without limit, but rather reduces with distance from the hyperbolic fixed point.

9.2 Invariance of the LCS

We now turn our attention to the assertion that LCS are invariant. Invariance is one of the defining characteristics of stable and unstable manifolds for autonomous sys-

tems, and hence the similarities between LCS and stable/unstable manifolds discussed previously, as well as the apparent invariance of the LCS observed in the applications, warrant a further study of this issue.

The question of invariance in relation to LCS contains two more subtle features that must be mentioned with regard to this matter. In the seminal paper of Haller [Haller 2000], LCS are defined as surfaces that are *always* repelling. It clearly follows that a surface that is always repelling will have no flux across it, and is necessarily invariant. However, the method he proposed for discovering these surfaces, namely the FTLE method, does not guarantee this property *a priori*. Haller regarded the FTLE method as a manner in which to approximate the "true" LCS that *are* invariant by definition, and posited that any flux across the LCS is an artifact of the FTLE approximation method. In contrast, Shadden's approach in [Shadden 2005] is to *define the LCS in terms of the FTLE*, and then to examine how invariant the LCS defined in this way actually are. The difference is somewhat semantic, but helps to explain some of the confusion as to whether LCS should be ascribed the property of invariance.

A second factor must also be considered. The group of Wiggins *et al.* have developed a separate method for extracting coherent structures in aperiodic flows called the "Distinguished Hyperbolic Trajectory" (DHT) method [Ide 2002]. The reader is referred to the references for a deeper study of this approach, however, the underpinning methodology is to first identify an "instantaneous stagnation point" (ISP) in the flow, the continuous motion of which defines a "distinguished hyperbolic trajectory" about which the linearized flow is maximally hyperbolic. The linearization about the ISP provides the linear subspaces that provide initial guides along which to search for the global stable and unstable manifolds. These manifolds are then declared to be the important structures in the time-dependent flow, and their time-dependence is obtained by advecting them forward in time using the given velocity field. The question of whether to use the FTLE approach or the DHT approach is largely a matter of preference; however, we have found that in analyzing geophysical flows, the DHT method has not been as effective because of the need to identify ISP's

which for many flows of interest are not Gaililean-invariant, or as is often the case, do not exist. The crucial point, though, is that in the DHT method the resulting time-dependent LCS are advected by the flow, and hence by definition, are invariant material surfaces. The development of this DHT method for extracting LCS, in which the LCS *are* invariant by definition, provides some additional confusion as to the invariance of the LCS for the FTLE-LCS method.

As mentioned previously, Shadden has provided a bound on the flux rate across an LCS, and has also verified numerically for an oceanic flow that flux across the LCS is almost negligible and falls within the numerical uncertainty of the calculation. The numerical results have led Haller to suggest (in conversation) that perhaps the flux estimate is not sharp, and that perhaps further analysis will reveal that FTLE-LCS are indeed invariant.

In this section, we will now present an example for which the FTLE-LCS is clearly not invariant – there is unambiguous flux across the LCS. Before presenting the example, we hasten to say that the Shadden flux estimate is not violated for this example. The example is a "pathological" case in which the underlying velocity field is smooth, but nevertheless has large temporal and spatial gradients. It is hoped that the example will be instructive in many ways. Beyond simply settling the question of the invariance of the FTLE-LCS, the example provides an indication of why a theory for LCS in time-dependent flows *must* admit flux across the LCS; *an invariant LCS may quickly become an irrelevant LCS.*

Example: Consider the flow in the xy-plane prescribed by

$$\dot{x} = 0.4 \tanh 10(x - 0.5t) \tag{9.18}$$

$$\dot{y} = 0\,. \tag{9.19}$$

This flow is only cheaply two-dimensional; the y-coordinate of each trajectory remains constant, and we need only consider the evolution of $x(t)$. As shown in Figure 9.4(a), the $\dot{x}$-component of the velocity field has a sigmoidal shape in space

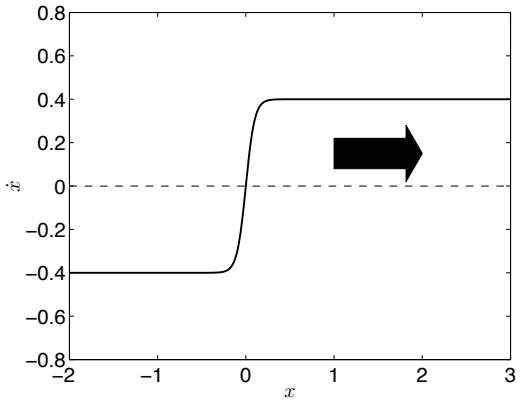

(a) Snapshot of the x-component of velocity as a function of the x-coordinate. In time, the sigmoidal velocity wave-front translates to the right.

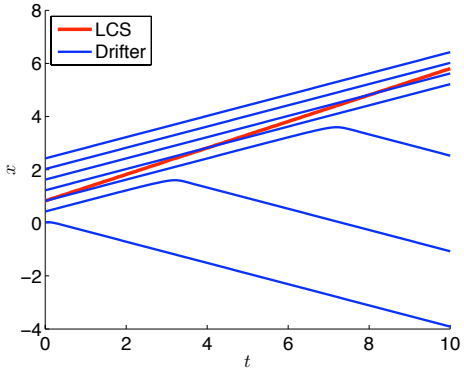

(b) The x-coordinate of drifter locations as a function of time are plotted in blue. The x-coordinate of the repelling LCS is shown in red, indicating the presence of flux across the LCS.

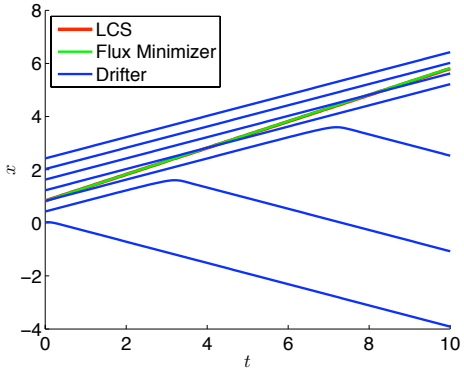

(c) The x-coordinate of the flux-minimizing path is plotted in green and coincides with the trajectory of the LCS. The flux minimizing path is derived in Section 9.2.1.

Figure 9.4: LCS in the flow of a sigmoidal wave front flow.

that propagates in time with constant speed in the direction of the positive x-axis. The important feature to notice is that the velocity profile translates with a velocity of 0.5 that is greater than the velocity of the fastest drifters in the flow (0.4). The factor of 10 in the argument of the tanh() function controls the steepness of the sigmoidal wave-front.

Computation of the FTLE for this flow reveals that the LCS is an infinite line parallel with the y-axis, that translates to the right, and in this way tracks the velocity front. In order to investigate flux across the LCS, we plot the x-location of the LCS

in relation to passive drifters in the flow. In Figure 9.4(b), where the horizontal axis is time, the x-coordinate of the LCS is shown to translate at a constant speed of 0.5 and tracks the wave-front. Drifter trajectories, however, are overtaken by the LCS, thus inducing continuous flux across the LCS. Clearly, the LCS in this example is not a material line, and not invariant.

It is instructive to compare the final location of the FTLE-LCS with a material line that originates at the same location. The LCS has translated to the right to keep pace with the velocity wave front which is the surface of greatest separation and the most important structure in the flow. The material line, on the other hand, is left behind in the wake of the flow. Thus, while an LCS that is materially advected remains invariant, it may no longer represent the important coherent structure in the flow. The implications of this observation are that we should not expect a theory that identifies coherent structures in aperiodic flows to provide LCS that are invariant, and the property of invariance may need to be sacrificed in order to ensure proper tracking of the relevant coherent structures. Further investigation of this example in the next section reveals the further subtle feature that the FTLE-LCS not only remains the relevant coherent structure in the flow, but does so in a manner that minimizes the flux. In other words, in this example, the FTLE-LCS provides the optimal tradeoff between tracking important structures and maintaining as much invariance as possible.

9.2.1 Motion of a Flux Minimizing Surface

Consider an arbitrary time-dependent velocity field, $\mathbf{f}(\mathbf{x}, t)$, defined on the plane, and suppose that $L^{t_0}(c)$ is a one-dimensional curve in the plane at time t_0 parametrized by $c \in [0, 1]$, and that $L^{t_1}(c)$ is another one-dimensional curve in the plane at time t_1 also parametrized by $c \in [0, 1]$, with $t_1 > t_0$. The situation is depicted in Figure 9.5.

We now propose the problem of choosing a one-parameter family of paths, $\mathbf{x}(c, t)$, in which the parameter c enumerates the paths, and each path is parametrized by time, t, so that $\mathbf{x}(c, t_0) = L^{t_0}(c)$, $\mathbf{x}(c, t_1) = L^{t_1}(c)$, and the flux induced by the velocity

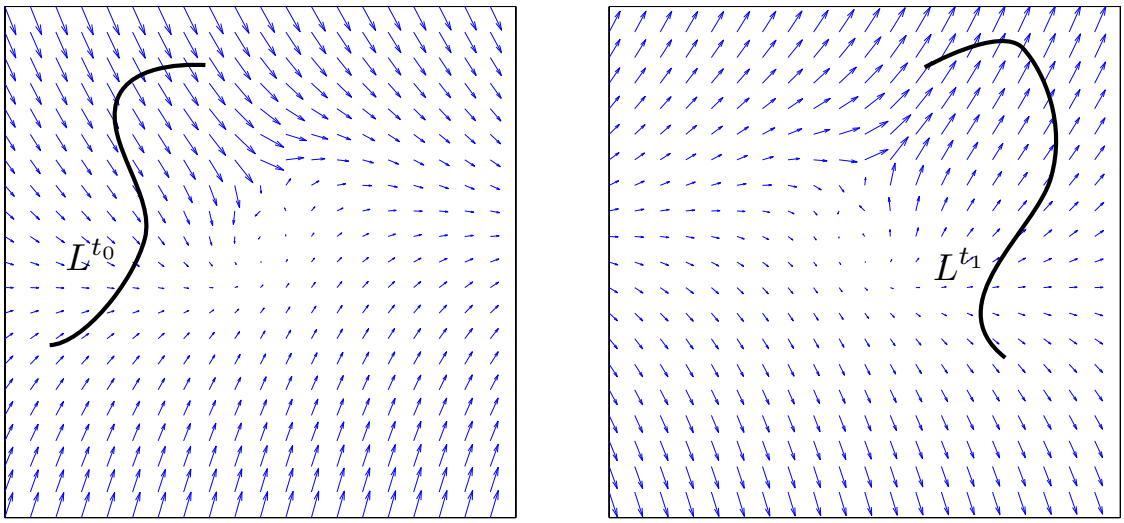

(a) time = t_0 (b) time = t_1

Figure 9.5: L^{t_0} is a curve shown at time t_0. L^{t_1} is a different curve at a later time, t_1. In the text, we derive the "most Lagrangian" transformation from L^{t_0} to L^{t_1} through the time-dependent velocity field.

field across each path is minimized. Said another way, we wish to choose the motion of the points located at $L^{t_0}(c)$ for $c \in [0,1]$ at time t_0 through the plane so that they arrive at corresponding points on the curve $L^{t_1}(c)$ for $c \in [0,1]$ at time t_1, and do so in a way that minimizes flux across each point. We can imagine the curve translating while morphing and changing its shape so that it arrives at $L^{t_1}(c)$ at time t_1 in a way that follows as closely as possible the underlying velocity field so as to reduce the flux. In this way, we hope to find "the most Lagrangian transformation" from L^{t_0} to L^{t_1}.

If $L^{t_1}(c) = \phi_{t_0}^{t_1}\left(L^{t_0}(c)\right)$ for all $c \in [0,1]$, where $\phi_{t_0}^{t_1}$ is the flow map for the velocity field $\mathbf{f}$, then the solution to the problem is obtained trivially by simply advecting the curve at time t_0 by the flow until time t_1. The advected curve will satisfy the boundary conditions, and will behave as a material line with precisely zero flux. However, for arbitrary placement of the final curve L^{t_1}, the motion of points along the curve must be found by applying a *variational principle*.

The motion of the point labelled by c is "most Lagrangian" when the flux integral

across the point is stationary:

$$\delta \int_{t_0}^{t_1} ||\dot{\mathbf{x}}(c,s) - \mathbf{f}(\mathbf{x}(c,s),s)||^2 \, ds = 0 \,. \tag{9.20}$$

The integrand can be considered a Lagrangian of the form:

$$L(\mathbf{x}, \dot{\mathbf{x}}, t) = ||\dot{\mathbf{x}}(c,t) - \mathbf{f}(\mathbf{x}(c,t),t)||^2 \,. \tag{9.21}$$

The Euler-Lagrange equations,

$$\frac{d}{dt}\left(\frac{\partial L}{\partial \dot{\mathbf{x}}}\right) - \frac{\partial L}{\partial \mathbf{x}} = 0 \,, \tag{9.22}$$

that arise from the variational principle yield

$$\ddot{\mathbf{x}} = \frac{\partial \mathbf{f}}{\partial t} + (\nabla \mathbf{f})' \cdot \mathbf{f} + (\nabla \mathbf{f} - (\nabla \mathbf{f})')\, \dot{\mathbf{x}} \tag{9.23}$$

for the second order dynamics of the flux minimizing point. The constants of integration are chosen to satisfy the boundary conditions.

The curve $\mathbf{x}(c,t)$ obtained by solving the boundary value problem is the path that moves through the time dependent velocity field from point $L^{t_0}(c)$ at time t_0, to the point $L^{t_1}(c)$ at time t_1, in such a way that it minimizes flux, and is most Lagrangian.

We have computed the flux-minimizing trajectory for the sigmoidal velocity-front example discussed earlier. The path of the flux-minimizing trajectory is plotted in Figure 9.4(c) and indicates that, for this example at least, the FTLE-LCS moves precisely along the trajectory that minimizes flux. Although the LCS is not invariant, it allows flux in order to retain its status as the important coherent structure, and does so in a manner that is optimal with respect to minimizing flux.

An added point to make here is that these findings indicate a manner in which to efficiently solve for the approximate motion of the LCS. If the location of the LCS is computed at time t_0, and at a much later time t_1, then the motion of the LCS during the interval of time (t_0, t_1) can be interpolated using the evolution of the

the flux minimizing curve. This ostensibly saves computation, since a large grid of trajectories no longer needs to be integrated at each time step, and improves upon the procedure of simply advecting the LCS by the velocity field which we have seen in the example can become largely inaccurate.

9.3 Equations of Motion for the LCS

In all the examples of the FTLE-LCS method provided in previous chapters, the time-dependence of the LCS is obtained by computing the location of the LCS at many time steps, and then animating the resulting frames to learn the motion of the LCS. This requires the computation of the FTLE over the entire region at many time steps, and the time-dependence of the LCS is an emergent feature extracted from the computed data. In this section, we address the time-dependence of the LCS in a different manner. In particular, we ask the question: "Given a velocity field, $\mathbf{f}(\mathbf{x}, t)$, and any needed derivatives, can we write evolution equations for the motion of the LCS?" If so, we will then, in principle at least, be able to solve for the motion of the LCS by direct integration of their deterministic equations of motion, without having to compute the FTLE everywhere and then extracting the apparent motion of the LCS.

In the discussion that follows we will proceed to derive equations of motion for the LCS and thus answer this question affirmatively. Unfortunately, however, the resulting equations of motion do not simplify to just a few explicit terms, but contain many terms defined up to quadrature that place a shadow over their utility for numerical computations. Nevertheless, we proceed with the analysis because (a) the idea of obtaining direct equations of motion for the LCS is intrinsically attractive, is worthy in its own merit, and if it can be done, must be done,[3] (b) simplification of the equations of motion (by approximation, for example) may in fact lead to more

[3]The author first started this calculation while visiting the Carlsberg Insititute, the former home of Niels Bohr, in Copenhagen, Denmark, and while discouraged that the calculations did not lead to a simple result, learned from Bohr's grandson, Tomas Bohr, of the long pages and pages of calculations that Bohr provided for his first gold-medal winning paper, and thus took courage.

efficient routines for computing the evolution of the LCS, and (c) having the explicit equations of motion in hand, although not practical for computations *per se*, may provide a breach through which we can attempt to provide further theoretical progress in proving definitive properties of the LCS. With regard to this last point, it is hoped that, just as Picard's iteration is seldom used for numerically integrating ordinary differential equations, but is nevertheless a singularly invaluable tool for proving existence and uniqueness of solutions, the evolution equations for the LCS may also provide insight and methods of proof for the properties of LCS. Certainly, the availability of equations of motion will spark new questions. For example, "Do the evolution equations follow from a variational principle in the velocity field?" At very least, the availability of evolution equations will allow expressions for quantities such as flux across the LCS (the relative motion between the LCS and the underlying flow) in terms of the primitive velocity fields, whereas we presently resort to numerical verifications at discrete time intervals.

In order to present the calculation that leads to the equations of motion, we appeal to the simple case of one-dimensional flow along the real line. This is manifestly the simplest flow we can consider, but it is nevertheless insightful since the same calculation for two-dimensional flow follows exactly analogous steps, albeit cluttered with more terms; and perhaps more importantly, for flow near a hyperbolic point, the flow is, as we have already seen, slaved to the unstable manifold so that for the purposes of understanding separation, we can think of the flow as essentially one-dimensional. In any case, we shall see that even though the flow is trivial, solving for the motion of the LCS may not be.

One-Dimensional Flow: We consider a time-dependent flow on the real line given by

$$\dot{x}(t) = f(x(t), t)\,. \tag{9.24}$$

The corresponding flow map ϕ that integrates points forward in the flow is

$$\phi_{t_0}^{t_0+T}(x_0) := x_0 + \int_0^T f(\phi_{t_0}^{t_0+s}(x_0), t_0+s)\, ds\,. \tag{9.25}$$

For one-dimensional flow, we identify the LCS as the point locations of greatest separation over the integration time T. That is, we must find the points that maximize the separation between two infinitesimally separated points. The scalar field $\sigma(x,t)$ provides the measure of separation:

$$\sigma(x,t) := \lim_{h\to 0} \frac{\phi_t^{t+T}(x+h) - \phi_t^{t+T}(x-h)}{2h} = \frac{d\phi_t^{t+T}(x)}{dx}\,. \tag{9.26}$$

We define the LCS as the locations $x_{LCS}(t)$ of locally maximal separation as measured by σ. Notice that in this setting, the LCS are now single points on the line that we may refer to individually as an "LCS point". Phrased differently, the point $x_{LCS}(t)$ simultaneously satisfies the conditions for a local maximum:

$$\frac{\partial\sigma(x_{LCS}(t),t)}{\partial x} = 0\,, \quad \text{and} \quad \frac{\partial^2\sigma(x_{LCS}(t),t)}{\partial x^2} < 0\,. \tag{9.27}$$

This condition is directly analogous to condition (3.1) for two-dimensional flow.

Our procedure is now to determine the motion of the LCS, $\dot{x}_{LCS}(t)$, by implicitly differentiating this constraint with respect to time. Our final goal is to write the evolution of the location of an LCS point in terms of the velocity field $f(x,t)$ and its derivatives. It will be incumbent upon us, during the evolution, to check that the condition on the second derivative of σ in (9.27) remains satisfied – otherwise, *ridges may become valleys.*

The time evolution of the LCS must be such that condition (9.27) remains satisfied along the path of the LCS point:

$$\frac{d}{dt}\left(\frac{\partial\sigma(x_{LCS}(t),t)}{\partial x}\right) = 0\,,$$

which, after expanding the material derivative, yields

$$\dot{x}_{LCS}(t) = -\frac{\frac{\partial^2 \sigma(x_{LCS},t)}{\partial x\, \partial t}}{\frac{\partial^2 \sigma(x_{LCS},t)}{\partial x^2}} = -\frac{\frac{\partial^3 \phi_t^{t+T}(x_{LCS})}{\partial x^2\, \partial t}}{\frac{\partial^3 \phi_t^{t+T}(x_{LCS})}{\partial x^3}}\,. \tag{9.28}$$

It now remains to write the required partial derivatives of the flow map with respect to space and time in terms of the velocity field, $f(x,t)$. Before doing so, we introduce some helpful shorthand notation. Let,

$$\phi_{m,n} := \left.\frac{\partial^{m+n} \phi_t^{t+T}}{\partial x^m \partial t^n}\right|_{x=x_0}, \tag{9.29}$$

and likewise

$$f_{m,n} := \left.\frac{\partial^{m+n} f}{\partial x^m \partial t^n}\right|_{\substack{t\,=\,t_0+s \\ x\,=\,\phi_{t_0}^{t_0+T}(x_0)}}. \tag{9.30}$$

Then, using

$$\phi_{t_0}^{t_0+T}(x_0) = x_0 + \int_0^T f(\phi_{t_0}^{t_0+s}(x_0), t_0+s)\, ds\,, \tag{9.31}$$

we derive the *variational equations* for the partial derivatives of the flow map. The variational equations are first order differential equations that must be integrated from an initial integration time 0, to the final integration time T, in order to obtain the value of the desired partial derivative. The variational equations for the first time derivatives are

$$\phi'_{1,0} = f_{1,0} \cdot \phi_{1,0} \qquad \phi_{1,0}(0) = 1 \tag{9.32}$$

and

$$\phi'_{0,1} = f_{0,1} + f_{1,0} \cdot \phi_{0,1} \qquad \phi_{0,1}(0) = 0\,. \tag{9.33}$$

The prime notation in these equations denotes differentiation with respect to a time of integration variable, s. Higher derivatives are written in terms of these partial derivatives. After some computation, we find that

$$\phi'_{1,1} = f_{1,1} + f_{2,0} \cdot \phi_{0,1} \cdot \phi_{1,0} + f_{1,0} \cdot \phi_{1,1} \qquad \phi_{1,1}(0) = 0\,, \tag{9.34}$$

$$\phi'_{3,0} = f_{3,0} \cdot [\phi_{1,0}]^3 + f_{1,0} \cdot \phi_{3,0} \qquad \phi_{3,0}(0) = 0\,, \tag{9.35}$$

and finally,

$$\phi'_{2,1} = f_{2,1} + f_{3,0} \cdot \phi_{0,1} \cdot [\phi_{1,0}]^2 + 2f_{2,0} \cdot \phi_{1,0} \cdot \phi_{1,1} + f_{1,0} \cdot \phi_{2,1} \qquad \phi_{2,1}(0) = 0\,. \tag{9.36}$$

In these derivations, we have used the fact that, by definition of LCS, $\phi_{2,0} = 0$ when evaluated on the LCS. These formulae provide a system of coupled ordinary differential equations written explicitly in terms of the velocity field, f, and its derivatives. Integrating these equations will provide the needed quantities in the formula for the evolution of the LCS point.

The complete set of coupled ordinary differential equations is reproduced here:

$$\phi'_{1,0} = f_{1,0} \cdot \phi_{1,0} \tag{9.37}$$

$$\phi'_{0,1} = f_{0,1} + f_{1,0} \cdot \phi_{0,1} \tag{9.38}$$

$$\phi'_{1,1} = f_{1,1} + f_{2,0} \cdot \phi_{0,1} \cdot \phi_{1,0} + f_{1,0} \cdot \phi_{1,1} \tag{9.39}$$

$$\phi'_{3,0} = f_{3,0} \cdot [\phi_{1,0}]^3 + f_{1,0} \cdot \phi_{3,0} \tag{9.40}$$

$$\phi'_{2,1} = f_{2,1} + f_{3,0} \cdot \phi_{0,1} \cdot [\phi_{1,0}]^2 + 2f_{2,0} \cdot \phi_{1,0} \cdot \phi_{1,1} + f_{1,0} \cdot \phi_{2,1}\,. \tag{9.41}$$

Notice that the equations are weakly coupled. In the first step, we may integrate the differential equations for $\phi_{1,0}$ and $\phi_{0,1}$ independently. With these in hand, we may compute $\phi_{1,1}$ and $\phi_{3,0}$. In the third and final step, we obtain $\phi_{2,1}$.

As derived previously in (9.28), the LCS point can then be advected using

$$\dot{x}_{LCS}(t) = -\frac{\phi_{2,1}}{\phi_{3,0}}\,. \tag{9.42}$$

We must also remember to monitor the value of $\phi_{3,0}$ to ensure that the second condition in the ridge definition remains satisfied.

Two-Dimensional Flow: The derivation of the evolution equations for the LCS in two-dimensional flow follows precisely analogous steps, except that the calculation is mired by many more terms generated in the expression – so many that it would be tiresome to use the resulting expressions in a numerical impementation. We provide the initial steps in the calculation here.

We consider a time-dependent flow in the plane given by

$$\dot{\mathbf{x}}(t) = \mathbf{f}(\mathbf{x}(t), t)\,, \tag{9.43}$$

for which the flow map is

$$\phi_{t_0}^{t_0+T}(\mathbf{x}_0) := \mathbf{x}_0 + \int_0^T \mathbf{f}(\phi_{t_0}^{t_0+s}(\mathbf{x}_0), t_0+s)\,ds\,. \tag{9.44}$$

and the FTLE is

$$\sigma(\mathbf{x}, t_0) := \frac{1}{2T} \ln \left[\lambda_{\max} \left[\left(\frac{d\phi_{t_0}^{t_0+T}(\mathbf{x})}{d\mathbf{x}} \right)^T \left(\frac{d\phi_{t_0}^{t_0+T}(\mathbf{x})}{d\mathbf{x}} \right) \right] \right]\,. \tag{9.45}$$

In this two dimensional flow, we can write the expression for the maximum eigenvalue explicitly:

$$\sigma(\mathbf{x}, t) = \frac{1}{2T} \ln \left[\frac{1}{2} \left(\phi_{1,x}^2 + \phi_{2,y}^2 + \sqrt{\phi_{1,x}^4 - 2\phi_{1,x}^2\phi_{2,y}^2 + \phi_{2,y}^4 + 4\phi_{1,y}^2\phi_{2,x}^2} \right) \right]\,, \tag{9.46}$$

where, for instance, $\phi_{1,x}$ represents the partial derivative of the first component of ϕ with respect to x. For further notational convenience, it will be helpful to denote partial differentiation of σ using subscripts also, so that

$$\sigma_{xxy} := \frac{\partial^3 \sigma}{\partial x^2 \partial y}\,, \tag{9.47}$$

for example.

LCS are defined as the ridges in the scalar field $\sigma(\mathbf{x}, t)$. To mathematically define "ridges", we will need to compute both the gradient of $\sigma(\mathbf{x}, t)$:

$$\nabla\sigma(\mathbf{x}, t) := \begin{bmatrix} \sigma_x \\ \sigma_y \end{bmatrix} , \tag{9.48}$$

and the Hessian:

$$\Sigma(\mathbf{x}, t) := \begin{bmatrix} \sigma_{xx} & \sigma_{xy} \\ \sigma_{xy} & \sigma_{yy} \end{bmatrix} . \tag{9.49}$$

The Hessian, $\Sigma(\mathbf{x}, t)$, has a minimum eigenvalue:

$$\lambda_{\mathbf{n}}(\mathbf{x}, t) = \lambda_{\min}\left[\Sigma(\mathbf{x}, t)\right] = \frac{1}{2}\left(\sigma_{xx} + \sigma_{yy} - \sqrt{\sigma_{xx}^2 - 2\sigma_{xx}\sigma_{yy} + \sigma_{yy}^2 + 4\sigma_{xy}^2}\right) , \tag{9.50}$$

with a corresponding eigenvector

$$\mathbf{n}(\mathbf{x}, t) = \begin{bmatrix} \sigma_{xx} - \sigma_{yy} - \sqrt{\sigma_{xx}^2 - 2\sigma_{xx}\sigma_{yy} + \sigma_{yy}^2 + 4\sigma_{xy}^2} \\ 2\sigma_{xy} \end{bmatrix} . \tag{9.51}$$

With these definitions of $\mathbf{n}$ and $\lambda_{\mathbf{n}}$ in hand, we can now define a point on the LCS as any point $\mathbf{x}_{LCS}$, for which the following two conditions are satisfied:

$$\nabla\sigma(\mathbf{x}_{LCS}, t) \cdot \mathbf{n}(\mathbf{x}_{LCS}, t) = 0 , \quad \text{and} \quad \lambda_{\mathbf{n}}(\mathbf{x}_{LCS}, t) < 0 . \tag{9.52}$$

These two conditions ensure that the point $\mathbf{x}_{LCS}$ lies on a ridge in the scalar field σ. At such a point, the eigenvector, $\mathbf{n}$, has the property that it is a vector normal to the LCS.

The evolution of the LCS is determined by finding precisely the motion that preserves the LCS condition:

$$\frac{d}{dt}\left[\nabla\sigma(\mathbf{x}_{LCS}, t) \cdot \mathbf{n}(\mathbf{x}_{LCS}, t)\right] = 0 . \tag{9.53}$$

Condition (9.53) is a single scalar equation for the two unknown components of $\dot{\mathbf{x}}_{LCS} = [\dot{x}_{LCS}, \dot{y}_{LCS}]$. In order to solve for $\dot{x}_{LCS}$ and $\dot{y}_{LCS}$, we must introduce a second condition. We choose to impose the condition that points on the LCS move only in a direction orthogonal to the LCS.[4] This is ensured by

$$\nabla\sigma \cdot \dot{\mathbf{x}}_{LCS} = 0\,. \tag{9.55}$$

Together, conditions (9.53) and (9.55) allow us to solve for the motion of the LCS. As before, we must always ensure that the minimum eigenvalue, $\lambda_{\mathbf{n}}$, remains negative during the evolution.

Expanding the derivative of condition (9.53) yields

$$\frac{\partial}{\partial t}\left(\nabla\sigma \cdot \mathbf{n}\right) + \dot{\mathbf{x}}_{LCS} \cdot \left(\Sigma\,\mathbf{n}\right) + \dot{\mathbf{x}}_{LCS} \cdot \left([\mathrm{D}\mathbf{n}]'\,\nabla\sigma\right) = 0\,.$$

Before solving for the components of $\dot{\mathbf{x}}_{LCS}$, we introduce one further simplification. Recall that $\mathbf{n}$ is an eigenvector of Σ corresponding to the eigenvalue $\lambda_{\mathbf{n}}$. Thus,

$$\frac{\partial}{\partial t}\left(\nabla\sigma \cdot \mathbf{n}\right) + \lambda_{\mathbf{n}}\left(\dot{\mathbf{x}}_{LCS} \cdot \mathbf{n}\right) + \dot{\mathbf{x}}_{LCS} \cdot \left([\mathrm{D}\mathbf{n}]'\,\nabla\sigma\right) = 0\,.$$

Finally, solving for the velocity of the LCS that satisfies the constraints yields

$$\dot{x}_{LCS} = \sigma_y \frac{A}{B} \tag{9.56}$$

$$\dot{y}_{LCS} = -\sigma_x \frac{A}{B}\,, \tag{9.57}$$

[4] An alternative condition is that the velocity of a point on the LCS, in the direction tangential to the LCS, is equal to the tangential velocity of the underlying velocity field:

$$\nabla\sigma \cdot \dot{\mathbf{x}}_{LCS} = \nabla\sigma \cdot \mathbf{f}\,, \tag{9.54}$$

which yields a slightly different result.

where

$$A := \frac{\partial}{\partial t}\left(\nabla\sigma \cdot \mathbf{n}\right) , \tag{9.58}$$

$$B := \sigma_x(\lambda_{\mathbf{n}} n_2 + \sigma_x n_{1,y} + \sigma_y n_{2,y}) - \sigma_y(\lambda_{\mathbf{n}} n_1 + \sigma_x n_{1,x} + \sigma_y n_{2,x}) . \tag{9.59}$$

Recall that all the terms in this expression are defined in terms of σ and its derivatives. In turn, equation (9.46) provides an expression for σ in terms of the flow map ϕ. The end result is that we can write an expression of the form

$$\dot{\mathbf{x}}_{LCS} = F[\phi] , \tag{9.60}$$

where F is a known function of ϕ and its partial derivatives.

Finally, the values of these partial derivatives can be computed using the variational equations as described for the case of one-dimensional flow, yielding evolution equations of motion for points on the LCS that can, in principle, be computed *a priori* from the underlying velocity field $\mathbf{f}(\mathbf{x}, t)$. Some of the terms in these equations simplify because we can impose the condition that the terms are evaluated on the LCS. Even so, it is bitterly clear at this point that the number of terms has become unwieldy, and we must resort to computer algebra or approximations before proceeding further.

This situation is not without parallel. The study of sensitivity analysis of ODE and DAE systems results in similar sets of equations. One potentially promising step forward on the numerical front is the possible incorporation of automatic differentiation methods developed by Barrio that are based on Taylor Series approximations, and are designed expressly for problems of this type [Barrio 2006].